scientific reports

Check for updates

OPEN

The IgLON family of cell adhesion molecules expressed in developing neural circuits ensure the proper functioning of the sensory system in mice

Katyayani Singh[1]✉, Mohan Jayaram[1], Arpana Hanumantharaju[1], Tambet Tõnissoo[2], Toomas Jagomäe[1,3], Kaie Mikheim[1], Srirathi Muthuraman[1], Scott F. Gilbert[4], Mario Plaas[3], Michael K. E. Schäfer[5,6,7], Jürgen Innos[1], Kersti Lilleväli[1,8], Mari-Anne Philips[1] & Eero Vasar[1]

Deletions and malfunctions of the IgLON family of cell adhesion molecules are associated with anatomical, behavioral, and metabolic manifestations of neuropsychiatric disorders. We have previously shown that IgLON genes are expressed in sensory nuclei/pathways and that IgLON proteins modulate sensory processing. Here, we examined the expression of IgLON alternative promoter-specific isoforms during embryonic development and studied the sensory consequences of the anatomical changes when one of the IgLON genes, *Negr1*, is knocked out. At the embryonal age of E12.5 and E13.5, various IgLONs were distributed differentially and dynamically in the developing sensory areas within the central and peripheral nervous system, as well as in limbs and mammary glands. Sensory tests showed that *Negr1* deficiency causes differences in vestibular function and temperature sensitivity in the knockout mice. Sex-specific differences were noted across olfaction, vestibular functioning, temperature regulation, and mechanical sensitivity. Our findings highlight the involvement of IgLON molecules during sensory circuit formation and suggest Negr1's critical role in somatosensory processing.

Keywords IgLON, NEGR1, LSAMP, PNS, DRG, Sensory processing

Sensory processing organizes sensation from the environment and encodes such input into primary bodily responses. This recognition, encoding, and organization requires precise communication between the central and peripheral nervous system. The peripheral nervous system (PNS) is a nexus of sensory circuits outside the brain and spinal cord consisting of cranial, spinal nerves, and ganglia for relaying neural signals between the central nervous system and effector organs[1]. The PNS provides the neurological basis of sensory perception, processing, and it contributes to other functions such as emotions, cognition, and reproduction[2,3]. A vertebrate's sensory framework originates from two distinct embryonic cell populations: the neural crest cells and a set of thickened ectodermal placodes[4]. During morphogenesis, these sensory precursors undergo tightly coordinated, mutual signaling interactions that organize and direct cells to build functional circuits with their intended targets[5,6].

In recent years, sensory processing deficits (SPD) have attained significant attention as an intrinsic contributor to the progression and severity of neuropsychological illnesses. While poorly addressed by contemporary treatment strategies, SPD represents abnormalities in the encoding and processing of sensory stimuli that

[1]Department of Physiology, Institute of Biomedicine and Translational Medicine, University of Tartu, 19 Ravila Street, 50411 Tartu, Estonia. [2]Institute of Molecular and Cell Biology, University of Tartu, Vanemuise 46-221, Ria 23-204, 51010 Tartu, Estonia. [3]Laboratory Animal Centre, Institute of Biomedicine and Translational Medicine, University of Tartu, 14B Ravila Street, 50411 Tartu, Estonia. [4]Department of Biology, Swarthmore College, Swarthmore, PA, USA. [5]Department of Anesthesiology, University Medical Center of the Johannes Gutenberg-University, 55131 Mainz, Germany. [6]Focus Program Translational Neurosciences, Johannes Gutenberg-University Mainz, 55131 Mainz, Germany. [7]Research Center for Immunotherapy, Johannes Gutenberg-University Mainz, 55131 Mainz, Germany. [8]The Centre of Estonian Rural Research and Knowledge, 48309 Jõgeva Alevik, Estonia. ✉email: katyayani.micro@gmail.com

hinder the daily functioning of individuals. SPD causes a sensory burden on patients and is a characteristic of neuropsychiatric conditions, including autism, attention deficit hyperactivity disorder, major depression, schizophrenia, Parkinson's, and Alzheimer's disease[7,8]. These include hyper- or hypo-reactivity to sensory inputs that result in under-responsiveness and/or over-responsiveness to stimuli, such as the tactile abnormalities in autism and the lower sensitivity towards high and low temperatures that major depression patients often exhibit. SPD can be an early indicator of illness, appearing before core symptoms such as mood changes, social problems, and cognitive deterioration. Indeed, impairments related to sensory system functioning may serve as predictive biomarkers for certain neuropsychiatric disorders[9]. Studying sensory processing phenotypes in animal models could be essential to understanding the underlying etiology of neuropsychiatric disorders across the full range of human well-being.

The IgLON superfamily of cell adhesion molecules consists of five glycosylated membrane-anchored proteins that have been shown to be involved in coordinating brain development and sensory functions[10–13]. Moreover, these proteins have also been associated with several neuropsychiatric disorders, including major depression, schizophrenia, autism, bipolar disorder, alcohol abuse, intellectual disabilities, and metabolic disorders such as obesity[14–18]. This superfamily contains five proteins: opioid-binding cell adhesion molecule (IgLON1/OPCML), neurotrimin (IgLON2/NTM), limbic-system associated membrane protein (IgLON3/LSAMP), neuronal growth regulator 1 (IgLON4/NEGR1), and IgLON5. Recent studies have also indicated the involvement of IgLON4 and IgLON5 in the progression of neurodegenerative disorders[19–21]. When genes of IgLON family members were knocked out of the mouse genome, the homozygous deficient mice were found to have several neuropsychological behavior impairments related to mood, social functioning, and cognition. In addition, the knockouts of these genes caused a wide spectrum of anatomical aberrations that included ventricular enlargements, reductions in brain volume, depletion of parvalbumin-positive inhibitory interneurons in the hippocampus, as well as monoaminergic impairments and metabolic disturbances corresponding to several neuropsychiatric conditions[10,22–29].

Alternative isoforms *1a/1b* regulate the expression of the Lsamp, Ntm, and Opcml proteins, and a single promoter system regulates *Negr1* expression. The mRNAs for the alternative isoforms and *Negr1*can be detected in sensory cortices, sensory relay centers, and associative areas[10,12,13,30]. Moreover, our previous study showed the expression of IgLONs in the murine neural crest and the developing central nervous system. At E11.5, expression of IgLON transcripts started appearing from a few cranial ganglia and in limb buds[12]. Major milestones of the sensory-peripheral system development, like sensory placodes, nuclei, ganglia, limb digits, cartilage, and muscle formation, appear by E12.5-E13.5[31–33]. Therefore, we propose that IgLON molecules may play important roles in forming the complex sensory circuits that function in input signal processing for generating sensations, emotions, cognitive behaviors, and control of motor actions. In the present study, we aim to elucidate (1) the expression of IgLON genes in the developing sensory system at the mid-embryonic stage and (2) the effect of *Negr1* deletion on the sensory system processing.

Results

Distribution of IgLON family members in the developing sensory and peripheral nervous system in mouse

To investigate the expression patterns of IgLON family members isoforms (*Lsamp1a*, *Lsamp uni (universal probe)*, *Negr1*, *Ntm 1a*, *Ntm 1b*, *Opcml 1a*, and *Opcml 1b*) in the developing sensory system and PNS, we employed the whole-mount in situ hybridization of mouse embryo at different developmental stages (E12.5 and E13.5). At E12.5-E13.5, IgLONs *(Lsamp 1a*, *Lsamp uni*, *Negr1*, *Ntm 1a*, *Ntm 1b*, *Opcml 1a*, and *Opcml 1b)* were highly expressed throughout the developing central nervous system (CNS), including the telencephalic vesicles, diencephalon, mesencephalon, metencephalon, myelencephalon and in the spinal cord (Figs. 1A–N and 2A–N).

IgLONs exhibited robust bilateral expression along the length of the spinal cord (Figs. 1H–N and 2H–N). In contrast to other members, *Opcml 1a* mRNA was remarkably attenuated, primarily confined to the anterior region on both lateral sides of the spinal cord (Fig. 1M). In the developing spinal cord, *Lsamp uni*, *Negr1*, and *Ntm1a/b* specifically marked the roof plate region (Figs. 1I–K and 2I–K). While *Lsamp1a*, *Lsamp uni*, *Negr1*, and *Ntm1a/1b* displayed expression throughout the dorsal root ganglia (DRG) (Figs. 1H–L and 2H–L). At E12.5, *Opcml1b* displayed a comparatively higher degree of expression in thoracic DRG regions (Fig. 1N). However, the expression of *Opcml1a* in the DRG remained relatively lower than the other members (Figs. 1M and 2M). In the head region, various IgLON members (*Lsamp uni*, *Negr1*, *Ntm 1a*/*1b*, and *Opcml 1b*) exhibited distinct expression within the trigeminal (V) nerve pathway (Fig. 1B–E,G,B′–E′,G′). Additionally, *Lsamp1a*, *Negr1*, and *Ntm1a/b* were discernible within the facio-acoustic ganglion (VII/VIII) complex (Fig. 1A,C–E,A′,C′–E′), and in the nodose ganglion (X) *Negr1*, *Ntm1a*, and *Ntm1b* were present (Fig. 1C–E,C′–E′). A detailed overview of IgLON´s expression domains at E12.5 and E13.5 are depicted in Supplementary Tables 1 and 2.

In the developing eye, at E12.5, the expression of the *Lsamp1a* and *Lsamp uni* mRNA was observed in the lens primordia (Fig. 1A′,B′), and the *Negr1* signal was detected in the *orbicularis occuli* muscles of developing eyes (Fig. 1C′). However, by E13.5, distinct expression of *Lsamp1a* and weak expression of *Lsamp uni* were detected within the center of the lens, in contrast to the other probes, which exhibited only weak expression in the peripheral area of the lens, were observed (Fig. 2A′–G′). Additionally, we identified expression of *Negr1*, *Ntm 1b*, and *Opcml 1b* in the *orbicularis oculi* muscles (Fig. 2C′,E′,G′), while only diffuse expression was observed around the eye with probes to *Lsamp 1a*/*uni*, *Ntm 1b*, and *Opcml 1a*/*1b* (Fig. 2A′,B′,E′–G′). In the developing inner ear, expression was particularly strong in the dorsally located vestibular region for *Lsamp uni*, *Negr1*, and *Ntm 1b* (Fig. 1B,C,E,B′,C′,E′). Moving to the posterior of the ear, we noted strong expression of *Lsamp uni*, *Lsamp1a* and *Opcml 1a*, in comparison to *Negr1*, *Ntm1a/b*, and *Opcml1b* probes (Fig. 2A–G,A′–G′). Within the developing face, *Lsamp1a* and *Lsamp uni* were expressed in a restricted area of the ventral frontonasal region (Fig. 1A,B), whereas *Negr1* and *Opcml1b* were detectable in both maxillary and mandibular regions (Fig. 1C,G).

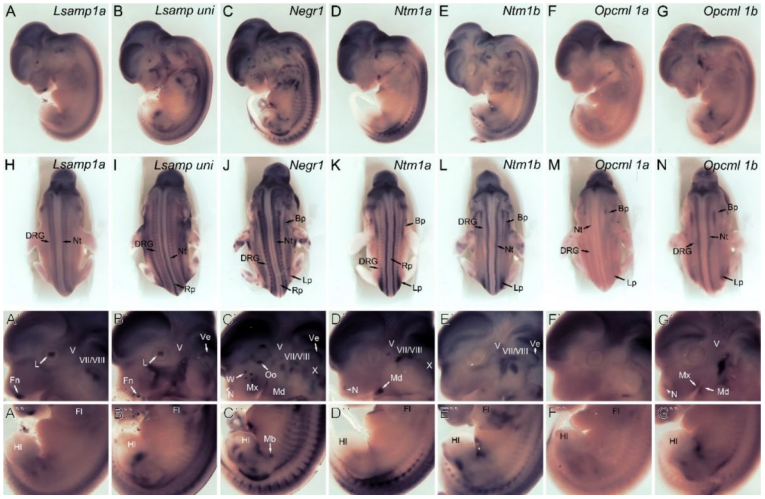

Fig. 1. At embryonic age, E12.5 IgLONs are expressed in mice's sensory precursor cells and spinal cord. Expression of *Lsamp 1a*, *Lsamp uni*, *Negr1*, *Ntm 1a*, *Ntm 1b*, *Opcml 1a*, and *Opcml 1b*, detected by whole-mount mRNA in situ hybridization. (**A**–**G**) lateral and (**H**–**N**) dorsal views of whole embryos. (**A**′–**G**′ and **A**″–**G**″) higher magnification images of the corresponding expression from the head and posterior body/hindlimb regions, respectively. *Bp* brachial plexus, *DRG* dorsal root ganglia, *Fl* forelimb, *Fn* frontonasal region, *Hl* hindlimb, *Ve* inner ear, *L* lens, *Lp* lumbosacral plexus, *Mb* mammary bud, *Md* mandibular, *Mx* maxilla, *N* nostril, *Nt* neural tube, *Oo orbicularis occuli*, *Rp* roof plate, *W* whiskers follicle, *V* trigeminal ganglion, *VII–VIII* facio-acoustic ganglion, *X* nodose ganglion.

Fig. 2. Distribution of IgLON family alternative promoters at embryonal age E13.5 in mice. Expression of *Lsamp 1a*, *Lsamp uni*, *Negr1*, *Ntm 1a*, *Ntm 1b*, *Opcml 1a*, and *Opcml 1b* mRNA was detected by whole-mount in situ hybridization wild-type embryos. (**A**–**G**) lateral and (**H**–**N**) dorsal views of whole embryos. (**A**′–**G**′ and **A**″–**G**″) higher magnification images of corresponding mRNA probe expression from head and limb regions, respectively. *DRG* dorsal root ganglia, *Fl* forelimb, *Hl* hindlimb, *Im* interdigital mesenchyme, *L* lens, *Mb* mammary bud, *N* nostril, *Nt* neural tube, *Ol* olfactory lobe, *Oo orbicularis occuli*, *Rp* roof plate, *W* whiskers follicle.

Ntm1a was only seen in the mandibular region (Fig. 1D). Moderate expression of *Negr1*, *Ntm1a*, *Ntm1b*, and *Opcml1b* mRNA was observed in the nostrils (Figs. 1C,D,G,C′,D′,G′ and 2C,E,G). At E12.5, in the snout`s whisker pad, we observed complementary expression between *Lsamp uni*- around the developing follicles and *Negr1* only at the whisker's follicles (Fig. 1B,C,B′,C′). As development progressed to E13.5, we observed profound expressions of *Lsamp1a*, *Lsamp uni*, *Ntm1a*/*b*, and *Opcml1a*/*b*, particularly around developing follicles (Fig. 2A′,B′,D′–G′). Specifically, *Negr1* and *Lsamp 1a* were present in whisker follicles, with *Negr1* mRNA being expressed distally and *Lsamp 1a* proximally (Fig. 2A′,C′).

Most of the IgLONs were expressed in the developing limb buds in distinct regions at E12.5: *Lsamp 1a* and *Opcml 1b* were observed in the proximal part of developing hindlimbs (Fig. 1A,G,A″,G″), *Lsamp uni* was

primarily expressed in the central part of hindlimbs (Fig. 1B,I,B″), and *Ntm1b* was detected in the posterior part of hindlimbs (Fig. 1E,E″). *Negr1* mRNA was detectable in the smaller structural units of the developing hindlimb (Fig. 1C,C″). Similarly, *Lsamp uni*, *Negr1* and *Ntm1b* were also expressed in various regions of the forelimb (Fig. 1B,C,E,B″,C″,E″). Notably, *Ntm1b* was specifically localized to the tips of digits in the forelimb (Fig. 1E,E″), while *Negr1* was observable in the interdigital mesenchyme (Fig. 1C). However, at E13.5, IgLONs exhibit variable expression patterns in different regions and a common feature was their expression in the interdigital mesenchyme (Fig. 2A–G,A″–G″). Notably, *Lsamp1a* and *Lsamp uni* displayed broader expression in both the forelimbs and hindlimbs compared to the earlier developmental stage at E12.5 (Fig. 2A,B,A″,B″). Interestingly, *Ntm1a* was expressed anteriorly in the narrow area of the central part of the forelimbs and both anterior and posterior regions of the central part of the hindlimbs (Fig. 2D,D″). IgLON gene expression was also observed around the developing mammary glands. We observed the presence of *Lsamp1a/uni*, *Ntm1b* and *Opcml1b* (Fig. 2A″,B″,E″,G″) in the regions around the mammary buds, while *Negr1* was specifically expressed within the mammary buds (Figs. 1C″ and 2C″). Furthermore, the expressions of *Negr1*, *Ntm 1a*, *Ntm 1b Opcml 1a*, and *Opcml 1b* were observed in presumptive brachial and lumbosacral plexuses or in the adjacent developing skeleton (Figs. 1J–N and 2J–N).

Analysis of sensory processing in the *Negr1* (IgLON 4): deficient mouse model

The developmental expression of IgLONs over the sensory organs, peripheral ganglia, and the spinal cord suggests the involvement of IgLONs in sensory and PNS functions. High expression of *Negr1* (IgLON4) mRNA in the developing forelimb and hindlimb interdigital mesenchyme, whiskers follicles, DRG, spinal cord, and in the caudal extremity of the neural tube and tail bud (Fig. 3A–C) prompted us to investigate the functioning of the somatosensory system in response to sensory stimuli in *Negr1*$^{-/-}$ mice.

Body weight was measured from a cohort of female and male *Negr1*$^{-/-}$ mice compared to their littermate Wt controls every week from the age of 2 months until the end of the experiments, i.e., age of 5 months. Three-way repeated-measures ANOVA was used to analyze the body weights of male and female mice. The analysis showed a significant effect of sex ($F(1, 76) = 704.7$; $p < 0.0001$), monthly age ($F(3, 76) = 51.05$; $p < 0.0001$), genotype ($F(1, 76) = 7.2$; $p = 0.008$) and sex X genotype interaction effects ($F(1, 76) = 24.02$; $p < 0.0001$) (Fig. 3D; Supplementary Table 3). We also performed Two-Way Repeated-Measures ANOVA separately for males and females to estimate the clear post hoc effects for each month for both the tested sexes. Male mice weighed more on average than females throughout early adulthood. In this cohort, no significant weight difference existed between genotypes in any of the measured months for the male mice. On the other hand, female *Negr1*$^{-/-}$ mice showed significant weight differences at the age of 4 ($p = 0.02$) and 5 ($p = 0.04$) months, as observed in Bonferroni's post hoc test report with Two-Way ANOVA.

The olfactory modality is one of the most important sensory systems by which mice explore the world. General olfactory function was tested using a buried pellet test. The buried pellet test relies on the natural

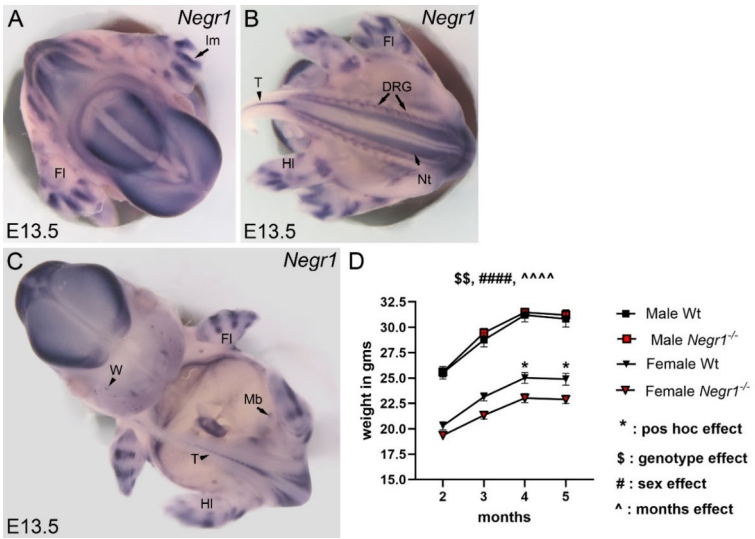

Fig. 3. *Negr1* mRNA is expressed in developing sensory organs and body weight dynamics of adult *Negr1*$^{-/-}$ and wild-type male and female mice cohort used in the study. (**A**–**C**) Whole-mount in situ hybridization for *Negr1* in wild-type (Wt) embryos at E13.5 revealed strong expression in interdigital mesenchyme of developing forelimbs and hindlimbs, dorsal root ganglia, spinal cord, and tail region. (**A**) top, (**B**) bottom, (**C**) front view of whole-mount embryo. (**D**) Body weight dynamics of Wt and *Negr1*$^{-/-}$ male and female mice cohort used for the sensory testing. Two-way ANOVA and Three-way ANOVA with Bonferroni's post hoc test were used to detect significant effects of genotype, sex, and monthly age on body weight from 2 to 5 months of mice (n = 20 mice in each group). For all plots, data show means ± SEM. Significance is denoted as follows: * for significant post hoc comparisons, $ for genotype, # for sex and ^ for months effects, $^{*}p < 0.05$, $^{\$\$}p < 0.01$, $^{\#\#\#\#}p < 0.0001$. *DRG* dorsal root ganglia, *FL* forelimb, *HL* hindlimb, *T* the caudal extremity of the neural tube in the tail region.

inclination of the animal to use olfactory cues for grazing. We first tested the palatability of the pellet by keeping a small amount of novel food pellets with mice 48 h before the experiment and found no difference between *Negr1*$^{-/-}$ mice and Wt in both male and female mice. Both strains consumed the entire sweetened cornflake pellets. To identify the possible genotype differences in olfactory function from female, male, *Negr1*$^{-/-}$ and Wt mice, we analyzed males and females separately with either *t*-test or Mann–Whitney U Test (according to normality distribution). We found no genotype difference in latency to find buried pellets or to pick food pellets kept on the surface (Supplementary Table 4). Thereafter, Two-way ANOVA with Bonferroni's post hoc test was used to check sex difference for olfactory function, and it was found that latency to find buried food pellets was affected significantly by sex ($F(1, 69) = 51.96$; $p < 0.0001$). Male mice from both genotypes took longer to find the buried food pellet compared to females (Fig. 4A). In a visual pellet test (pellet on surface test), no significant difference was found between both the sex and genotype, which excluded the possible influence of motivation on olfaction (Supplementary Fig. S1; Supplementary Tables 3 and 4).

Visual acuity was measured for optokinetic response, and we found no significant difference between *Negr1*$^{-/-}$ and Wt control groups in either male or female mice (Fig. 4B). During visual acuity tests, optokinetic stimulation was given by rotating large drums overlaid with vertical black and white stripes at various spatial frequencies around the animals that had been placed in an elevated resting platform. While measuring the optokinetic responses, we noticed that *Negr1*$^{-/-}$ mice were falling off the platform within a few seconds before even starting the optokinetic stimulation. This precipitous falling indicated disturbances in vestibular senses or sense of equilibrium. Hence, we assessed the frequency of mice falling off the raised platform and kept the background color as grey. Male *Negr1*$^{-/-}$ mice fell off the platform significantly more often compared to the Wt mice ($p = 0.005$ analyzed by *t*-test). However, females did not fall off the platform. Two-way ANOVA showed significant sex ($F(1, 24) = 4.73$; $p = 0.03$) and genotype difference ($F(1, 24) = 7.72$; $p = 0.01$) in the frequency of falls (Fig. 4C).

Next, we examined somatosensory processing with sensations from cold and hot temperatures and mechanical stimuli. Cold temperature sensitivity was recorded with the cold plantar test through withdrawal latency time. No significant difference was found between genotypes or sexes (Fig. 4D). Both male and female mice displayed similar sensitivity towards cold stimuli. The hot-plate test was used to study nociception and thermal sensitivity by measuring the latency to flick or jump the hind paw. The Mann–Whitney test found significant genotype differences in females ($p = 0.01$), a similar trend was found in males ($p = 0.09$) in that direction, as estimated by the *t*-test. Likewise, Two-way ANOVA depicted a significant difference between genotypes ($F(1, 76) = 7.31$; $p = 0.008$). (Fig. 4E).

Mechanical sensitivity was analyzed for a paw withdrawal threshold using 2 g and 4 g Von-Frey hair filaments. We first checked paw withdrawal response with a series of consecutive Von-Frey filaments from 0.1 to 6 g. We found that mice started to respond to the filaments from 2 g, and at 4 g, the maximum paw withdrawal threshold was observed. Therefore, we decided to check paw withdrawal response at both 2 g and 4 g filaments. Initial

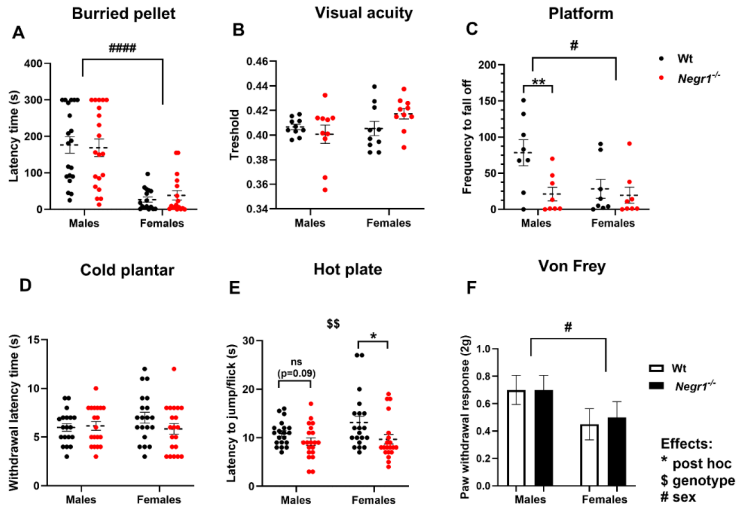

Fig. 4. Deletion of *Negr1* resulted in impaired sensory function in mice (**A**) olfactory function test by buried food pellet test, (**B**) visual acuity test using optometer (**C**) equilibrium/balance at heights test done by using the elevated platform for frequency to fall off (**D**) cold sensitivity is measured by cold plantar test and (**E**) thermal allodynia is measured by hot plate test (**F**) mechanical sensitivity by 2 g Von Frey filament. For all plots, data show means ± SEM. Differences between the genotypes were tested by *t*-test or Mann–Whitney test. Two-way ANOVA, with post hoc Bonferroni comparisons, was used to check sex effects within the genotype between groups. Significance is denoted as follows: and * for significant comparisons between genotypes; $^{*}p < 0.05$, $^{**}p < 0.01$, $^{***}p < 0.001$ and $^{\#}p < 0.05$, $^{\#\#\#\#}p < 0.0001$ for sex effects. Sample size was n = 20 in each group, i.e., each group containing male Wt (n = 20) and *Negr1*$^{-/-}$ (n = 20) mice, in female Wt (n = 20) and *Negr1*$^{-/-}$ (n = 20) mice, except n = 8–10 in each group for visual acuity and platform test.

statistical analysis did not show any genotype difference among male and female test mice. Two-way ANOVA revealed significant sex differences only with 2 g Von-Frey hair filament (F (1, 76) = 4.19; $P = 0.04$). More details on statistical results are shown (Fig. 4F; Supplementary Fig. S2; Supplementary Tables 3 and 4).

To further probe the multimodal sensory processing, we used combinations of different sensory modalities from somatic sensations (tactile, heat, cold, and vestibular) for sensorimotor evaluation. The Morris water was employed for the assessment of the impact of water temperatures on swimming speed in *Negr1*$^{-/-}$ males and females and male *Lsamp*$^{-/-}$ mice with their control Wt mice. The maze trials were conducted at three different water temperatures: cold (10 °C), lukewarm (22 °C), and warm (32 °C).

Two-way ANOVA analysis showed that male *Negr1*$^{-/-}$ mice had significant genotype differences (F (1, 90) = 27.19; $p < 0.0001$) and temperature effect differences (F (2, 90) = 13.30; $p < 0.0001$; Fig. 5A) at swimming speed. Post hoc comparisons exhibited clear significant differences at different water temperatures observed in male mice at 22 °C ($p = 0.02$) and at 32 °C ($p = 0.05$). Surprisingly, female *Negr1*$^{-/-}$ mice showed only a temperature effect (F (2, 90) = 4.41; $p = 0.01$) and no genotype effects were seen in post hoc analysis of swimming speed at any of the swimming water conditions (cold, lukewarm or warm). Moreover, in this experimental model, we tested another IgLON-deficient mouse line, *Lsamp*$^{-/-}$ male mice, to examine the effect of water temperature differences on swimming speed. Results from *Lsamp*$^{-/-}$ mice exhibited significant genotype effects (F (1, 85) = 35.82; $p < 0.0001$). In contrast to *Negr1*$^{-/-}$ male mice, *Lsamp*$^{-/-}$ mice were swimming at the lower speed only at lower temperatures (10 °C $p < 0.0001$ and at 22 °C; $p = 0.003$) with (Fig. 5A,B; Supplementary Table S4).

Negr1 and *Lsamp* exhibited contrasting expression patterns during embryonic development.The complementary expression patterns were seen near the whisker follicular areas, at developing limbs, and the semi-circular duct area (Fig. 5C). All these areas effects sensorimotor functions. Altogether, results indicated a stronger sex difference in *Negr1*$^{-/-}$ mice towards somatosensory performances, and male *Negr1*$^{-/-}$ and *Lsamp*$^{-/-}$ mice showed affected sensitivities for water temperature in swimming (sensorimotor task), where the LSAMP deficiency affected the functioning more at a lower temperature as compared to *Negr1*$^{-/-}$ mice.

Gene expression analysis for primary sensory neuron regulation in the DRG of *Negr1*$^{-/-}$ mice

Our results demonstrated a high expression of *Negr1* in DRG. Hence, we examined whether *Negr1* deletion in mice affects mRNA expression of temperature-sensing receptor channels in DRG. We used DRG from 5-month-old male and female *Negr1*$^{-/-}$ mice and performed qPCR analysis to reveal mRNA expression for the thermosensors; Transient receptor potential channels (*TRP*): *Trpv1*, *Trpa1*, *Trpm3*, *Trpm8*, α-form of calcitonin gene-related peptide (*CGRP*), and Substance P (*SP*). All these sensors are expressed in a large subset of C and

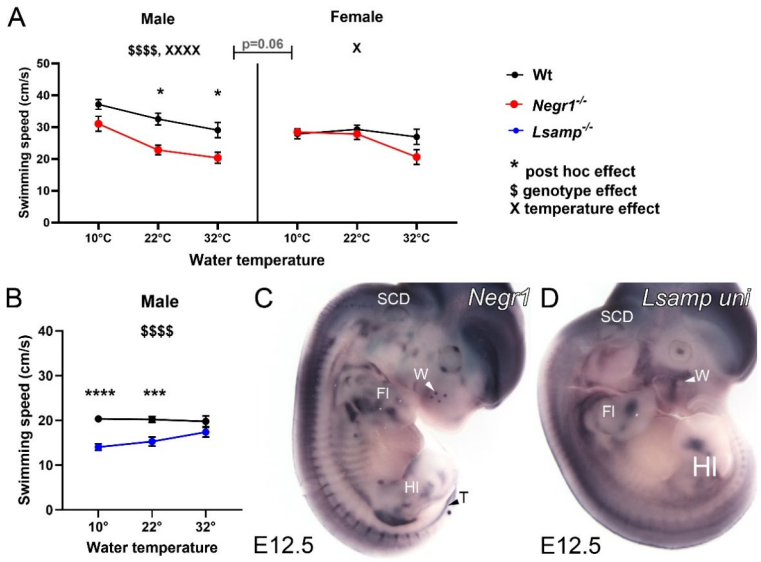

Fig. 5. Effect of water temperature on swimming speed in *Negr1*$^{-/-}$ and *Lsamp*$^{-/-}$ mice; and representative illustration showing complementary activity of *Negr1* and *Lsamp uni* mRNA probes in developing sensory precursors. (**A**) The difference in swimming speed of *Negr1*$^{-/-}$ males, *Negr1*$^{-/-}$ females with Wt mice and (**B**) in *Lsamp*$^{-/-}$ males at different water temperatures (10 °C, 22 °C, 32 °C) (**C**) Complementary expression of *Negr1* and *Lsamp uni* probes were observed in developing whiskers and in limb precursors at E12.5 embryo. For the plot, data show means ± SEM. Two-way ANOVA was used with post hoc Bonferroni comparisons to check genotype and water temperature effects within the genotype between groups. Three-way ANOVA was conducted only with *Negr1*$^{-/-}$ male and female data sets to check sex differences among all the groups. Significance is denoted as follows: $ for post hoc comparisons between genotypes; $$$$ $p < 0.0001$, X for temperature difference, X $p < 0.05$, XXXX $p < 0.0001$ temperature effects and *for post hoc from Two-way ANOVA *$p < 0.05$, ***$p < 0.001$, ****$p < 0.0001$. The sample size was n = 16–18 in each group. *FL* forelimb, *HL* hindlimb, *SCD* semi-circular duct, *T* the caudal extremity of the neural tube, *W* whisker follicle.

Aδ sensory neurons of mouse DRG, and they are responsible for detecting and providing signal responses at different temperature-mediated stimuli[34]: *Trpv1* for thermal hyperalgesia is evoked by > 43 °C heat stimuli; *Trpa1* senses for cold hyperalgesia; *Trpm3* becomes activated at 33 to 37 °C; and *Trpm8* is activated by moderate cooling at 24 °C.

To identify the genotype differences in DRG samples for sensory-related genes, we first analyzed males and females separately with either a *t*-test or Mann–Whitney U Test (according to normality distribution) to compare Wt and *Negr1*$^{-/-}$ groups. However, genotype-related differences were not observed (Fig. 6A–F, Supplementary Table 3).

Next, we checked sex differences using Two-way ANOVA and found significant sex differences for *Trpv1* ($F(1, 29) = 5.82$; $p = 0.02$) and *Trpa1* gene ($F(1, 30) = 9.92$; $p = 0.003$). Bonferroni post hoc comparisons indicated higher mRNA expression of *Trpv1* in female Wt samples as compared to male Wt and *Negr1*$^{-/-}$ DRG samples. Similarity was relative mRNA expression of *Trpa1* in female *Negr1*$^{-/-}$ samples higher as compared to male *Negr1*$^{-/-}$ DRG samples; details of statistical values can be found in Supplementary Tables 5 and 6.

Discussion

We report that IgLONs are expressed in the developing sensory system and its neuronal pathways within the CNS and PNS. Functional consequences of these developmental associations were demonstrated by the dysfunctional somatosensory processing in the *Negr1*$^{-/-}$mice. In recent years, genetic studies from neuropsychiatric consortia have correlated IgLON cell adhesion molecules with several cross-disorder neuropsychiatric conditions, highlighting them, especially NEGR1, as promising therapeutic targets. Impairments of sensory processing are among the most debilitating manifestations of many neuropsychiatric disorders and often comprise an independent variable from the affective and cognitive domains[35]. Both genetic and environmental cues play major roles in the development and accurate function of sensory circuits[36]. Indeed, while IgLON molecules have been known for having significant functions during CNS development and behavior, very little has been known about the role of IgLONs in the formation and functioning of the sensory system. Therefore, we examined various sensory system processing modalities in a neuropsychiatric mouse model (*Negr1*$^{-/-}$) in an RDoC protocol that investigates sensory processing dysfunctions through genetic, environmental, and behavioral modes[9].

Our current results support our previous findings of adult mice, wherein we showed the expression levels of IgLON transcripts in various sensory nuclei within the CNS and in peripheral tissues[10,11]. These investigations demonstrated that specific sets of neurons use alternative IgLON promoters during brain development and suggested that alternative IgLON promoter transcripts may also have significant functions in diverse developmental processes. The present study extends IgLONs role in functioning to the development of the sensory system and PNS. PNS nerves relay afferent sensory signals from primary sensory organs to the brain and spinal cord for further processing and thereafter transmit motor signals to the face, limbs, and musculature[1,37]. Our results demonstrate that IgLONs are expressed in developing primary sensory organs such as the eye lens,

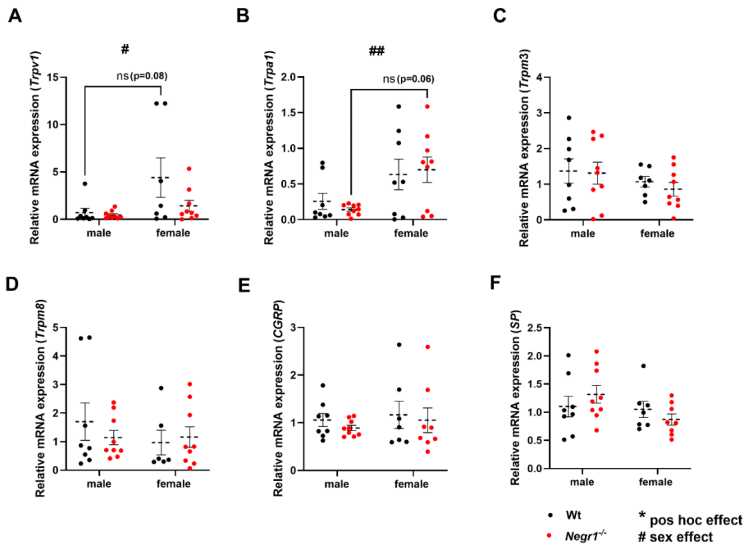

Fig. 6. Relative mRNA expression levels of transient receptor potential channels and neuropeptides in DRG of Wt and *Negr1*$^{-/-}$ mice from both males and females. (**A**) *Trpv1*, (**B**) *Trpa1*, (**C**) *Trpm3*, (**D**) *Trpm8*, (**E**) *CGRP* (Calcitonin gene-related peptide), and (**F**) *SP* (Substance P). For all plots, data show means ± SEM. Differences between the genotypes were tested by *t*-test or Mann–Whitney test. Two-way ANOVA, with post hoc Bonferroni comparisons, was used to check sex and interaction effects within the genotype between groups. Significance is denoted as follows: and * for post hoc significant comparisons between genotypes; $^{*}p < 0.05$, and $^{\#}p < 0.05$, $^{\#\#}p < 0.01$ for sex effects. The sample size was n = 10 in each group, i.e., each group containing male and female of Wt and *Negr1*$^{-/-}$ mice; outliers were identified using the ROUT test.

nearby ocular muscle, inner ear, semicircular duct, cochlear area, facial region (maxillary and mandibular), and the vibrissa area of mice embryo. The PNS is thought to have dual progenitors, as neural crest cells and the ectodermal placodes both generate cranial sensory ganglia and primary sense organs[38,39].

At embryonic stages E12.5 and E13.5, most of the sensory placodes have formed and are differentiating their specific nerves. The expression of IgLON indicates that these molecules are most likely involved in the differentiation of sensory neurons during the formation of these sensory placodes. It has been suggested previously that IgLON molecules in developing chick embryos may be necessary for the communication and segregation of neuroepithelium and neural crest cells, marking their crucial role during PNS formation[40].

Each sensory cranial ganglia defines somatosensory and visceral sensory neurons that execute specific functions. Our results thereby relate the activity of IgLONs with developing cranial nerve pathways of the trigeminal (V), facial-acoustic (VII–VIII), jugular, and nodose ganglia (Figs. 1 and 2). Trigeminal nerves transmit sensation from touch, pain, and temperature modalities of facial muscles that include sensory afferents from ophthalmic (cornea, conjunctiva, nasal mucosa, upper eyelids, and forehead), maxillary (middle facial region, lower eyelids and upper teeth), whereas mandibular area (oral mucosa, tongue and lower teeth) have both sensory and motor nerves that are required for bite, chewing, swallowing and affected by proprioceptive impulses[41]. Physiological and anatomical studies revealed a closed relationship between cranial nerves V and VII carrying sensation of taste[42]. It has been noted that *Lsamp*, *Ntm*, and *Negr1* have a stronger expression in the developing semicircular duct of the inner ear as well as in VII-VIII ganglia, suggesting that these IgLON molecules may be essential for the execution of vestibular functions in vertebrates. *Ntm* and *Negr1* were also expressed in the nodose ganglia (X), which helps in sensing vital organs to control homeostasis by regulating blood pressure, heart rate, digestion, and breathing. IgLONs are also involved in the development of other somatosensory neurons from neck and trunk situated in DRG (Fig. 7), where axons range from the periphery to the ventral part of the spinal cord and can respond to a wide variety of sensory cues (mechanical, proprioceptive, nociceptive, pruriceptive and thermoreceptive)[43]. Several studies have revealed insights into the IgLON adhesion molecule's expression and function for the outgrowth of DRG and spinal cord neurons[13,44–46]. Both during development and adulthood, IgLONs are specifically expressed in the barrel cortex, which is the primary sensory projection area of the cortex processing whisker sensation. The *Lsamp*1b promoter activity is specific and strong in layers 4 and 6 of most of the primary sensory areas of the cortex[10]; the expression of *Opcml 1a/b* and *Ntm 1b*is also strongly highlighted in the barrel cortex area[12]. Strong expression of *Negr1* at whisker follicles and complementary expression of *Lsamp* in the area surrounding whisker follicles draws attention to our previous studies, which showed that both *Negr1*- and *Lsamp*-deficient mice exhibit significantly reduced whiskers trimming and have several social and cognitive impairments at the behavior level[22,26]. One of the recent studies performed with male *Negr1*$^{-/-}$mice displayed impaired affective discrimination and olfactory sensory processing with reduced olfactory bulb neurogenesis, indicating that neuronal alteration in the olfactory region can influence affective recognition[47].

Our somatosensory function studies on *Negr1*$^{-/-}$ mice expand the developmental findings. Differences in the weight dynamics of males, females, and between genotypes in the tested cohort appear to be mediated, at least in part, by the *Negr1* gene function that regulates the hypothalamic circuits involving metabolism control and energy expenditure[27,48]. Male *Negr1*$^{-/-}$ mice display increased falling-off frequency from raised platforms, suggesting that the Negr1 molecule affects the state of equilibrium. A decreased heat threshold was observed in *Negr1*$^{-/-}$mice using the hot-plate test, and swimming at different water temperatures indicates the involvement of Negr1 with thermo-sensing mechanisms. Thermal sensitivities were also observed in other rodent models of neuropsychiatric disorders[49–51]. Male and female *Negr1*$^{-/-}$ mice show differences in preference for swimming at

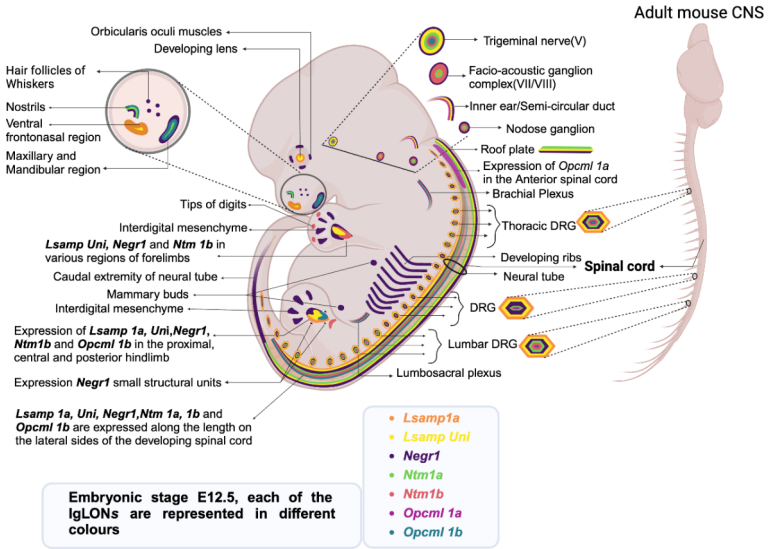

Fig. 7. Schematic illustration of IgLON molecule transcripts expressions at embryonic age E121.5 in developing sensory and peripheral structures in mice. (Image is created using Biorender).

different water conditions; male mice have slower speeds in warm and lukewarm water. This may be an indication that female mice are unaffected by water temperature for swimming and rather prefer to float in a relaxed state. These results suggest that male mice may have pronounced impairments in sensorimotor pathways and these pathways are diverged in males and females. Another mouse model from IgLON family molecules, *Lsamp*$^{-/-}$ shows sensitivity towards lower water temperatures (10 °C and 22 °C), displaying that *Lsamp*-deficiency-related genotype difference in swimming speed was exaggerated in cold water and diminished in warm water. These results suggest that *Lsamp*$^{-/-}$ mice are more susceptible to cold, and LSAMP protein could enable coping in hypothermia conditions. In our previous study, we have shown that *Lsamp* 1b promoter activity is prevalent in the sensory nuclei and primary cortex areas, covering major nuclei within afferent somatosensory, auditory, and visual pathways, additionally both *Lsamp*1a and 1b promoters are expressed in brain areas involved in the processing of gustatory and olfactory information[10]. Surprisingly, no major sensory deficiencies have been detected in *Lsamp*-deficient mice. In an earlier experimental series with *Lsamp*-deficient mice, we showed that their swimming speed is significantly lower[22]. Later, we specified that this phenotype was not dependent on either isolation stress or enriched environmental conditions[52]. It is known that water temperature affects swimming performance and that sex differences in body mass may explain thermal preferences[53,54].

These behavioral test results collectively converge to show impairments of somatosensation in IgLON-deficient mice. To further explore a possible mechanistic pathway involving these sensory processing deficits, we explored the expression of thermo-sensors and sensory neuropeptides responsible for promoting excitation or sensitization of the primary sensory nerve fibers of DRG. The main outcome was sex-specific differences for *Trpv1* and *Trpa1*, where the relative expression was found to be higher in *Negr1*$^{-/-}$ female mice as compared to their counterpart male. Increased levels of *Trpv1* could also indicate possible causes of male-female differences in the somatosensory and movement changes in *Negr1*$^{-/-}$ mice. Studies report that *Trpv1*channels are also expressed in the CNS, specifically in the hypothalamus, limbic areas, dopaminergic neurons of the striatum, midbrain, astrocytes, and microglia, and possess an expanded function beyond thermal sensation like somatosensory and movement responses[55–57]. Spatial transcriptomics in human primary afferents recently revealed that women express a higher number of differentially regulated genes in *Trpa1*-containing fibers than men[58]. It has also been shown that TRPV1 and TRPA1 channels trigger the release of CGRP and SP, inducing neurogenic inflammation[59,60].

Although we didn't find any difference at the gene level in *Negr1*$^{-/-}$ mice compared to Wt, this can be explained by the fact that we have performed experiments without noxious, heat, or cold activation of the channels. Our limitation in this work was that DRGs were collected to measure the basal levels of these sensory regulators in the sensory neurons of *Negr1*$^{-/-}$ mice. Thus, the precise type of thermos-sensor activation or mechano-sensing piezo channels and their link to nociception associated with the NEGR1 protein needs further clarification and suggestions for future research. Future studies might be needed to understand if sex chromosomes differentially influence CAMs during the critical early stages of development in male and female mice. The observed sex-specific differences could indicate the participation of the NEGR1 in the sexual dimorphic activation of sensory pathways. Broadly, these differences emphasize the paramount importance of including female mice cohorts in preclinical studies and could benefit the potential personalized or sex-specific therapeutic interventions in the future. To some extent, this work fulfills the current proposal of the RDoC matrix concerning missing sensory domains despite their prevalence in several neuropsychiatric disorders.

In conclusion, we demonstrate that IgLONs are expressed in developing primary sensory organs and peripheral sensory ganglia, indicating the dynamic role of IgLONs in mechanisms underlying complex sensory processing. Our results demonstrated the importance of Negr1 molecules in somatosensory processing. It is, therefore, likely that IgLONs play critically important roles that allow the nervous system to sense, integrate, and respond to the changing world of external sensory cues.

Materials and methods

Animals

Wild-type C57BL/6N (Scanbur, Karl-slunde, Denmark) mice were used for in situ hybridization. Male and female *Negr1*$^{+/+}$ mice (hereinafter referred to as wild type (Wt) and their *Negr1*-deficient littermates (*Negr1*$^{-/-}$), described previously[48], and male *Lsamp*$^{+/+}$ (hereinafter referred to as wild type (Wt) (*Lsamp*$^{+/+}$) mice and *Lsamp*-deficient littermates (*Lsamp*$^{-/-}$) as described[22], in F2 background ((129S5/SvEvBrd × C57BL/6N) × (129S5/SvEvBrd × C57BL/6N)) were used in the present study. Mice were group-housed in standard laboratory cages measuring 42.5 (L) × 26.6 (W) × 15.5 (H) cm, with 10 animals per cage in the animal colony, at 22 ± 1 °C under a 12:12 h light/dark cycle (lights off at 19:00 h). A 2 cm layer of aspen bedding (Tapvei, Estonia) and 0.5 l of aspen nesting material (Tapvei, Estonia) were used in each cage and changed every week. Water and food pellets (R70, Lactamin AB, Sweden) were available *ad libitum*. Breeding and the maintenance of the mice were performed at the animal facility of the Institute of Biomedicine and Translational Medicine, University of Tartu, Estonia. The use of mice was conducted in accordance with the regulations and guidelines approved by the Laboratory Animal Centre at the Institute of Biomedicine and Translational Medicine, University of Tartu, Estonia. All animal procedures were conducted in accordance with the European Communities Directive (2010/63/EU) with permit (No. 150, 27 September 2019 & No. 234, 30 December 2022) from the Estonian National Board of Animal Experiments. We confirm this study is reported in accordance with the ARRIVE (Animal Research: Reporting of In Vivo Experiments) guidelines as outlined at https://arriveguidelines.org.

In situ hybridization

The *Lsamp 1a* and *universal (uni)* probes were prepared as described[10]. Mouse cDNA fragment specific for *Ntm 1a* (285 bp), *Ntm 1b* (500 bp), *Opcml 1a* (492 bp), *Opcml 1b* (514 bp) and *Negr1* (650 bp) transcripts were cloned from a cDNA pool of C57BL/6 mouse brain and inserted into pBluescript KS+ vector (Stratagene, La

Jolla, CA). We used primers (containing restriction sites) for *Ntm 1a*, *1b*, *Opcml 1a*, *1b* and *Negr1*as described[12]. Whole-mount in situ hybridization on 4% paraformaldehyde-fixed embryos was carried out using digoxigenin-UTP (Roche) labeled sense and antisense RNA probes as described previously[12]. Three replicates of in situ hybridization with 3–4 embryos per probe in each replicate were used in these experiments.

Behavior testing

All the experiments were conducted between 9:00 and 17:00. The mice were 17–18 weeks at the beginning of the behavior tests. The tests were conducted in the following order: visual acuity, buried pellet test, platform test, cold planter, von Frey test, and hot plate test. The same cohort of mice was used for the series of tests, and the mice were brought into the experiment room 45–60 min prior to habituation before all the tests.

Visual acuity analysis

To measure visual acuity, a virtual optomotor task (OptoMotry, Cerebral Mechanics Inc., Alberta, Canada) was used, and the measurement was performed according to the previously described paper[61]. Briefly, animals were placed on an elevated platform (18.5 cm) in the center of a virtual rotating cylinder displaying vertical bars to stimulate the optomotor response (OMR). The width of the bars in the rotating cylinder was made progressively smaller and the tracking behavior of the animals was recorded. The minimal width of the bars that induced tracking behavior is a surrogate measure of the maximal spatial frequency resolution of the mice. Clockwise rotation was detected by the left eye, and anticlockwise rotation by the right eye. Visual acuity data are presented as the means of clockwise and anticlockwise testing.

Olfactory test (buried pellet test)

A buried pellet test was conducted to assess olfactory performance. Mice were introduced to the novel feed pellet (Nestle-Honey and Nut Cornflakes) 48 h before the test and were observed after 24 h for palatability, and the novel feed was consumed in all the cohort cages. Prior to the test, mice were starved for 16–18 h before the test while water was still provided. The test was performed under 300 lx. The test cage was prepared using Plexiglass cages measuring 26 (L) × 20 (W) × 14 (H) cm with ~ 3 cm bedding was used. One intact cornflake pellet weighing 0.1 to 0.2 g was placed under 1 cm of sawdust bedding in one corner of the test cage. The subject mice were placed in the test cage, and the latency time to uncover the pellet was recorded. If a mouse did not uncover the pellet within the test duration i.e. 300 s, the experiment was terminated, and mice were given a latency of 300 s. Subsequently, the mouse was removed, and the test was repeated with the same strategy, except the pellet was placed on the surface in the center of the test cage to exclude possible motor disorders or alterations in food motivation. The time latency of the first bite of the pellet was noted. After every test, a fresh cage with bedding was used throughout the experiment. reintroduced into the same cage with a pellet on the surface of the bedding. Now, the time of the first bite was noted. Cages were replaced with new bedding for each mouse. Mice were then provided with *ad-libitum* feed.

Platform test

To check balance through falling-off effects from elevated platforms, the internal setup for placing mice in the Optomotry by Cerebral Mechanics Inc was used. During the test, mice were placed on a platform at a height of 18.5 cm and a diameter of 11.5 cm. The platform was at the center of 4 digital screens, and white light was displayed on all the screens. Mice were placed on the platform for 300 s, and the time of each fall was noted. Frequency to fall off was calculated as the total time of each fall per total number of falls in 300 s (F = a + b+…/N; where a, b…correspond to the time at which mice are falling off and N is the total number of falling off).

Cold plantar

The cold response threshold (cold allodynia) to cold stimulus was tested with dry ice. For this test, a 5 ml syringe was used with the tip cut off, retaining only the barrel and the plunger. The dry ice was then powdered and filled into the syringe, and compressed against a flat surface till the plunger could no longer be pushed smoothly. Mice were placed in a 2000 ml jar; the investigator then brought the jar above eye level and placed the dry ice-filled syringe against the center of the left hind paw. The dry ice was pushed 20 to 30 mm above the barrel before placing it against the hind left paw. The time of left paw flicking since the contact with dry ice was noted as pain response time.

Von Frey test

Mechanical or tactile response threshold to mechanical sensitivity was tested manually using Von Frey filaments. We tested different von Frey filaments with random mice, and it was noted that the minimum force applied in 2 g and 4 g filaments elicited an immediate paw withdrawal response. Therefore, mechanical sensitivity was tested using 2 g and 4 g filaments with all the tested mice. During the test, a metal mesh plate 91(L) × 20 (W) cm elevated at 50 cm was placed above the working table as it provided full access to the paws. The filaments were tested on one of the front and hind paws; during the procedure, the filaments were pushed against the paws perpendicularly for 5 s. The withdrawal was scored as 1, and no response was scored as 0.

Hot plate

Thermal or heat response to thermal sensitivity (thermal allodynia) or pain response to heat was tested with a Stuart Large Capacity Hot plate. The plate was maintained at 55 °C, and mice were placed with the tail touching the surface of the plate. The time of flick or lick of the hind paws was noted as a response. Some mice jumped before paw flicking or licking, which was also considered as a response.

Swim test at different temperatures

Both male and female *Negr1*$^{-/-}$ mice and male *Lsamp*$^{-/-}$ mice were used in this test paradigm. Weight measurements were taken one day before the test. On the day of the test, mice were placed in the behavior room for one hour before the start of the test for acclimatization. Morris water maze was used for the mice swimming test; water was kept at 40 cm deep at all temperatures, and mice were allowed to swim for 60 s in water at 10 °C, 22 °C, and 32 °C, respectively. A time gap of more than a 60-minute was given to mice for swimming tests at different water temperatures to allow body temperature recovery between trials. Importantly, the data for the *Lsamp*$^{-/-}$ line was collected earlier in a different vivarium setup, which is also why only male groups were used for the *Lsamp*$^{-/-}$ line. Nevertheless, the swimming speed test procedure was identical for both lines, except the analysis of swimming speed was done using recorded video and tracker through the TSE Systems (for *Lsamp*$^{-/-}$ line) and using the Etho Vision system (for *Negr1*$^{-/-}$ line). Due to the different detection systems, the overall swimming speed of the *Negr1*$^{-/-}$ line was 1.5–2 times higher than in *Lsamp*$^{-/-}$. The difference comes from the detection system (e.g., Etho Vision counts slight right- or left-turns as distance moves forward). Therefore, swimming speed data should be interpreted only by comparing different temperature conditions within one mouse line.

RT-qPCR analysis in mouse dorsal root ganglia (DRG)

Gene expression was calculated by two-step RT-qPCR (qPCR). Total RNA was extracted from DRG of adult male and female *Negr1*$^{-/-}$ mice samples by using Trizol reagent (Invitrogen) according to the manufacturer's protocol. First-strand cDNA was synthesized by using FIREScript RT cDNA Synthesis MIX with Oligo (dT) and Random primers (Solis BioDyne, Tartu, Estonia) according to the manufacturer's protocol.

In qPCR, we studied the relative gene expression of 6 genes having significance in primary sensory neuron regulation. The studied genes are transient receptor potential (TRP) channels: *Trpv1*, *Trpa1*, *Trpm3*, *Trpm8*, neuropeptides: Calcitonin gene-related peptide (*CGRP*), Substance P (*SP*) and two housekeeper genes, beta-actin (*ActB*) and *Hprt* were used for the relative analysis. The primer sequences used are:

*Trpv1*_F CAAGGCTCTATGATCGCAGG
*Trpv1*_R GAGCAATGGTGTCGTTCTGC
*Trpa1*_F ACAAGAAGTACCAAACATTGACACA
*Trpa1*_R TTAACTGCGTTTAAGACAAAATTCC
*Trpm8*_F GCTGTGGCCTCGTATCATTT
*Trpm8*_R GAGCAGCACATAGGCAAACA
*Trpm3*_F CTTTCGGACCCTCTACCA
*Trpm3*_R CCTCTTCCTCACGCTTCT
*Calca*_F ATAACAGCCCCAGAATGAAG
*Calca*_R CAATACTAAGAAGGATGCAAAT
*SP*_F TTTCTCGTTTCCACTCAACTGTT
*SP*_R GTCTTCGGGCGATTCTCTGC
*Hprt*_F GCAGTACAGCCCCAAAATGG
*Hprt*_R AACAAAGTCTGGCCTGTATCCAA

All reactions were done with a total volume of 10 µL, using 5 ng of cDNA, and to minimize possible error, four parallel replicates were made with each reaction. Real-time qPCR was performed using HOT FIREPol® EvaGreen® qPCR Supermix (Solis BioDyne). For qPCR detection, ABI Prism 7900HT Sequence Detection System with ABI Prism 7900 SDS 2.4.2 software (Applied Biosystems) was used. qRT-PCR data in the Figures is presented on a linear scale, calculated as $2-\Delta\Delta CT$, where ΔCT is the difference in cycle threshold (CT) between the target genes and the housekeeper gene.

Statistical analysis

Statistical analysis was performed using GraphPad Prism 10 software. All results are presented as means ± SEM. For statistical analysis of data, we used a two-tailed Student's *t*-test when the data exhibited normal distribution, and the Mann–Whitney *U* test when the dataset did not pass the normal distribution test or normal distribution could not be tested. When comparing more than two groups, multiple-comparison analysis of variance (ANOVA), 2-way ANOVA, or 3-way ANOVA was used with the Bonferroni post hoc multiple-comparison test. The numbers of animals/samples/statistical tests are indicated in the figure legends. Individual data points represent biological replicates. The differences were significant if the p-values were less than 0.05.

Data availability

The data that support the findings of this study are available upon written request to the corresponding author.

Received: 10 July 2024; Accepted: 17 September 2024
Published online: 30 September 2024

References

1. Catala, M. & Kubis, N. Gross anatomy and development of the peripheral nervous system. *Handb. Clin. Neurol.* **115**, 29–41. https://doi.org/10.1016/B978-0-444-52902-2.00003-5 (2013).
2. Baum, M. J. & Cherry, J. A. Processing by the main olfactory system of chemosignals that facilitate mammalian reproduction. *Horm. Behav.* **68**, 53–64. https://doi.org/10.1016/j.yhbeh.2014.06.003 (2015).

3. Burke, K. & Kobrina, A. Rodentia sensory systems. In *Encyclopedia of Animal Cognition and Behavior* (eds Vonk, J. & Shackelford, T. K.) (Springer, 2022). https://doi.org/10.1007/978-3-319-55065-7_765.
4. Francis-West, P. H., Ladher, R. K. & Schoenwolf, G. C. Development of the sensory organs. *Sci. Prog.* **85**, 151–173. https://doi.org/10.3184/003685002783238852 (2002).
5. Collado, M. S. *et al.* The postnatal accumulation of junctional E-cadherin is inversely correlated with the capacity for supporting cells to convert directly into sensory hair cells in mammalian balance organs. *J. Neurosci.* **31**, 11855–11866. https://doi.org/10.1523/JNEUROSCI.2525-11.2011 (2011).
6. Liu, X. *et al.* Roles of neuroligins in central nervous system development: Focus on glial neuroligins and neuron neuroligins. *J. Transl. Med.* **20**, 418. https://doi.org/10.1186/s12967-022-03625-y (2022).
7. Velasques, B. *et al.* Sensorimotor integration and psychopathology: Motor control abnormalities related to psychiatric disorders. *World J. Biol. Psychiatry* **12**, 560–573. https://doi.org/10.3109/15622975.2010.551405 (2011).
8. van den Boogert, F. *et al.* Sensory processing difficulties in psychiatric disorders: A meta-analysis. *J. Psychiatr. Res.* **151**, 173–180. https://doi.org/10.1016/j.jpsychires.2022.04.020 (2022).
9. Harrison, L. A., Kats, A., Williams, M. E. & Aziz-Zadeh, L. The importance of sensory processing in mental health: A proposed addition to the research domain criteria (RDoC) and suggestions for RDoC 2.0. *Front. Psychol.* **10**, 103. https://doi.org/10.3389/fpsyg.2019.00103 (2019).
10. Philips, M. A. *et al.* Lsamp is implicated in the regulation of emotional and social behavior by use of alternative promoters in the brain. *Brain Struct. Funct.* **220**, 1381–1393. https://doi.org/10.1007/s00429-014-0732-x (2015).
11. Vanaveski, T. *et al.* Promoter-specific expression and genomic structure of IgLON family genes in mouse. *Front. Neurosci.* **11**, 38. https://doi.org/10.3389/fnins.2017.00038 (2018).
12. Jagomäe, T. *et al.* Alternative promoter use governs the expression of IgLON cell adhesion molecules in histogenetic fields of the embryonic mouse brain. *Int. J. Mol. Sci.* **22**, 6955. https://doi.org/10.3390/ijms22136955 (2021).
13. Fearnley, S., Raja, R. & Cloutier, J. F. Spatiotemporal expression of *IgLON* family members in the developing mouse nervous system. *Sci. Rep.* **11**, 19536. https://doi.org/10.1038/s41598-021-97768-5 (2021).
14. Pan, Y., Wang, K. S. & Aragam, N. NTM and NR3C2 polymorphisms influencing intelligence: Family-based association studies. *Prog. Neuropsychopharmacol. Biol. Psychiatry* **35**, 154–160. https://doi.org/10.1016/j.pnpbp.2010.10.016 (2011).
15. Hyde, C. L. *et al.* Identification of 15 genetic loci associated with risk of major depression in individuals of European descent. *Nat. Genet.* **48**, 1031–1036. https://doi.org/10.1038/ng.3623 (2016).
16. Karis, K. *et al.* Altered expression profile of IgLON family of neural cell adhesion molecules in the dorsolateral prefrontal cortex of schizophrenic patients. *Front. Mol. Neurosci.* **11**, 8. https://doi.org/10.3389/fnmol.2018.00008 (2018).
17. Bernhard, F. *et al.* Functional relevance of genes implicated by obesity genome-wide association study signals for human adipocyte biology. *Diabetologia* **56**, 311–322. https://doi.org/10.1007/s00125-012-2773-0 (2013).
18 Viggiano, M. *et al.* Genomic analysis of 116 autism families strengthens known risk genes and highlights promising candidates. *NPJ Genom. Med.* **9**, 21. https://doi.org/10.1038/s41525-024-00411-1 (2024).
19. Raghavan, N. S., Vardarajan, B. & Mayeux, R. Genomic variation in educational attainment modifies Alzheimer disease risk. *Neurol. Genet.* **5**, e310. https://doi.org/10.1212/NXG.0000000000000310 (2019).
20 Abdi, I. Y. *et al.* Cross-sectional proteomic expression in Parkinson's disease-related proteins in drug-naïve patients vs healthy controls with longitudinal clinical follow-up. *Neurobiol. Dis.* **177**, 105997. https://doi.org/10.1016/j.nbd.2023.105997 (2023).
21. Lee, S. Y. *et al.* Phenotypic insights into anti-IgLON5 disease in IgLON5-deficient mice. *Neurol. Neuroimmunol. Neuroinflamm.* **11**, e200234. https://doi.org/10.1212/NXI.0000000000200234 (2024).
22. Innos, J. et al. Lower anxiety and a decrease in agonistic behaviour in Lsamp-deficient mice. *Behav. Brain Res.* **217**(1), 21–31. https://doi.org/10.1016/j.bbr.2010.09.019 (2011).
23. Mazitov, T., Bregin, A., Philips, M. A., Innos, J. & Vasar, E. Deficit in emotional learning in neurotrimin knockout mice. *Behav. Brain Res.317*, 311–318. https://doi.org/10.1016/j.bbr.2016.09.064 (2017).
24. Bregin, A. *et al.* Expression and impact of Lsamp neural adhesion molecule in the serotonergic neurotransmission system. *Pharmacol. Biochem. Behav.* **198**, 173017. https://doi.org/10.1016/j.pbb.2020.173017 (2020).
25. Singh, K. *et al.* Neuronal growth and behavioral alterations in mice deficient for the psychiatric disease-associated *Negr1* gene. *Front. Mol. Neurosci.* **11**, 30. https://doi.org/10.3389/fnmol.2018.00030 (2018).
26. Singh, K. *et al.* The combined impact of IgLON family proteins Lsamp and neurotrimin on developing neurons and behavioral profiles in mouse. *Brain Res. Bull.* **140**, 5–18. https://doi.org/10.1016/j.brainresbull.2018.03.013 (2018).
27. Singh, K. *et al.* Neural cell adhesion molecule *Negr1* deficiency in mouse results in structural brain endophenotypes and behavioral deviations related to psychiatric disorders. *Sci. Rep.* **9**, 5457. https://doi.org/10.1038/s41598-019-41991-8 (2019).
28. Kaare, M. *et al.* High-fat diet induces pre-diabetes and distinct sex-specific metabolic alterations in Negr1-deficient mice. *Biomedicines* **9**, 1148. https://doi.org/10.3390/biomedicines9091148 (2021).
29. Kaare, M. *et al.* Depression-associated *Negr1* gene-deficiency induces alterations in the monoaminergic neurotransmission enhancing time-dependent sensitization to amphetamine in male mice. *Brain Sci.* **12**, 1696. https://doi.org/10.3390/brainsci12121696 (2022).
30. Kimura, Y., Katoh, A., Kaneko, T., Takahama, K. & Tanaka, H. Two members of the IgLON family are expressed in a restricted region of the developing chick brain and neural crest. *Dev. Growth Differ.* **43**(3), 257–263. https://doi.org/10.1046/j.1440-169x.2001.00570.x (2001).
31. Martin, P. Tissue patterning in the developing mouse limb. *Int. J. Dev. Biol.* **34**(3), 323–336 (1990).
32. Kaufman MH. *The atlas of mouse development*. Third revised edition 1999, 525(Academic Press, San Diego, 1992).
33. Chen, V. S. et al. Histology atlas of the developing prenatal and postnatal mouse central nervous system, with emphasis on prenatal days E7.5 to E18.5. *Toxicol. Pathol.* **45**(6), 705–744. https://doi.org/10.1177/0192623317728134 (2017).
34. Rosenbaum, T., Morales-Lázaro, S. L. & Islas, L. D. TRP channels: A journey towards a molecular understanding of pain. *Nat. Rev. Neurosci.* **23**, 596–610. https://doi.org/10.1038/s41583-022-00611-7 (2022).
35. Perju-Dumbrava, L. & Kempster, P. Movement disorders in psychiatric patients. *BMJ Neurol. Open* **2**, e000057. https://doi.org/10.1136/bmjno-2020-000057 (2020).
36. Leighton, A. H. & Lohmann, C. The wiring of developing sensory circuits—From patterned spontaneous activity to synaptic plasticity mechanisms. *Front. Neural Circuits* **10**, 71. https://doi.org/10.3389/fncir.2016.00071 (2016).
37. Vermeiren, S., Bellefroid, E. J. & Desiderio, S. Vertebrate sensory ganglia: Common and divergent features of the transcriptional programs generating their functional specialization. *Front. Cell Dev. Biol.* **8**, 587699. https://doi.org/10.3389/fcell.2020.587699 (2020).
38. Baker, C. V. & Bronner-Fraser, M. Vertebrate cranial placodes I. Embryonic induction. *Dev. Biol.* **232**, 1–61. https://doi.org/10.1006/dbio.2001.0156 (2001).
39. Butler, S. J. & Bronner, M. E. From classical to current: Analyzing peripheral nervous system and spinal cord lineage and fate. *Dev. Biol.* **398**, 135–146. https://doi.org/10.1016/j.ydbio.2014.09.033 (2015).
40. Kimura, Y., Katoh, A., Kaneko, T., Takahama, K. & Tanaka, H. Two members of the IgLON family are expressed in a restricted region of the developing chick brain and neural crest. *Dev. Growth Differ.* **43**, 257–263. https://doi.org/10.1046/j.1440-169x.2001.00570.x (2001).
41. Walker, H. K. Cranial nerve V: The trigeminal nerve. In *Clinical Methods: The History, Physical, and Laboratory Examinations* 3rd edn (eds Walker, H. K. et al.) (Butterworths, 1990).

42. Sanders, R. D. The trigeminal (V) and facial (VII) cranial nerves: Head and face sensation and movement. *Psychiatry (Edgmont)* **7**, 13–16 (2010).
43. Meltzer, S., Santiago, C., Sharma, N. & Ginty, D. D. The cellular and molecular basis of somatosensory neuron development. *Neuron* **109**, 3736–3757. https://doi.org/10.1016/j.neuron.2021.09.004 (2021).
44. Gil, O. D. *et al.* Complementary expression and heterophilic interactions between IgLON family members neurotrimin and LAMP. *J. Neurobiol.* **51**, 190–204. https://doi.org/10.1002/neu.10050 (2002).
45. Sanz, R. L., Ferraro, G. B., Girouard, M. P. & Fournier, A. E. Ectodomain shedding of limbic system-associated membrane protein (LSAMP) by ADAM metallopeptidases promotes neurite outgrowth in DRG neurons. *Sci. Rep.* **7**, 7961. https://doi.org/10.1038/s41598-017-08315-0 (2017).
46. Smith-Anttila, C. J. A. *et al.* Identification of a sacral, visceral sensory transcriptome in embryonic and adult mice. *ENeuro* **7**, 0397. https://doi.org/10.1523/ENEURO.0397-19.2019 (2020).
47. Kim, K. H., Noh, K., Lee, J., Lee, S. & Lee, S. J. Neuronal growth regulator 1 modulates mouse affective discrimination by regulating adult olfactory neurogenesis. *Biol. Psychiatry Glob. Open Sci.* https://doi.org/10.1016/j.bpsgos.2024.100355 (2024).
48. Lee, A. W. *et al.* Functional inactivation of the genome-wide association study obesity gene neuronal growth regulator 1 in mice causes a body mass phenotype. *PLoS ONE* **7**, e41537. https://doi.org/10.1371/journal.pone.0041537 (2012).
49. Irie, F., Badie-Mahdavi, H. & Yamaguchi, Y. Autism-like socio-communicative deficits and stereotypies in mice lacking heparan sulfate. *Proc. Natl. Acad. Sci. U.S.A.* **109**, 5052–5056. https://doi.org/10.1073/pnas.1117881109 (2012).
50. Shi, M., Qi, W.-J., Gao, G., Wang, J.-Y. & Luo, F. Increased thermal and mechanical nociceptive thresholds in rats with depressive-like behaviors. *Brain Res.* **1353**, 225–233. https://doi.org/10.1016/j.brainres.2010.07.023 (2010).
51. Han, Q. *et al.* SHANK3 deficiency impairs heat hyperalgesia and TRPV1 signaling in primary sensory neurons. *Neuron* **92**, 1279–1293. https://doi.org/10.1016/j.neuron.2016.11.007 (2016).
52. Innos, J. *et al.* Deletion of the Lsamp gene lowers sensitivity to stressful environmental manipulations in mice. *Behav. Brain Res.* **228**, 74–81. https://doi.org/10.1016/j.bbr.2011.11.033 (2012).
53. Iivonen, K. S. *et al.* Relationship between fundamental motor skills and physical activity in 4-year-old preschool children. *Percept. Mot. Skills* **117**, 627–646. https://doi.org/10.2466/10.06.PMS.117x22z7 (2013).
54. Kaikaew, K., Steenbergen, J., Themmen, A. P. N., Visser, J. A. & Grefhorst, A. Sex difference in thermal preference of adult mice does not depend on presence of the gonads. *Biol. Sex Differ.* **8**, 24. https://doi.org/10.1186/s13293-017-0145-7 (2017).
55. Martins, D., Tavares, I. & Morgado, C. "Hotheaded": The role OF TRPV1 in brain functions. *Neuropharmacology* **85**, 151–157. https://doi.org/10.1016/j.neuropharm.2014.05.034 (2014).
56. Hudson, A. S., Kunstetter, A. C., Damasceno, W. C. & Wanner, S. P. Involvement of the TRPV1 channel in the modulation of spontaneous locomotor activity, physical performance and physical exercise-induced physiological responses. *Braz. J. Med. Biol. Res.* **49**(6), e5183. https://doi.org/10.1590/1414-431X20165183 (2016).
57. Serra, G. P., Guillaumin, A., Dumas, S., Vlcek, B. & Wallén-Mackenzie, Å. Midbrain dopamine neurons defined by TrpV1 modulate psychomotor behavior. *Front. Neural Circuits* **15**, 726893. https://doi.org/10.3389/fncir.2021.726893 (2021).
58. Tavares-Ferreira, D. *et al.* Spatial transcriptomics of dorsal root ganglia identifies molecular signatures of human nociceptors. *Sci. Transl. Med.* **14**, eabj8186. https://doi.org/10.1126/scitranslmed.abj8186 (2022).
59. González-Ramírez, R., Chen, Y., Liedtke, W. B. & Morales-Lázaro, S. L. TRP channels and pain. In *Neurobiology of TRP Channels* (CRC Press/Taylor & Francis, 2017)
60. Koivisto, A. P., Belvisi, M. G., Gaudet, R. & Szallasi, A. Advances in TRP channel drug discovery: From target validation to clinical studies. *Nat. Rev. Drug Discov.* **21**, 41–59. https://doi.org/10.1038/s41573-021-00268-4 (2022).
61. Seppa, K. *et al.* Liraglutide, 7,8-DHF and their co-treatment prevents loss of vision and cognitive decline in a Wolfram syndrome rat model. *Sci. Rep.* **11**, 2275. https://doi.org/10.1038/s41598-021-81768-6 (2021).

Author contributions

Conceptualization: K.S., K.L., T.J., J.I., E.V.; Methodology: K.S., M.J., T.J., J.I., A.H., K.M.; Analysis: K.S., K.L., T.J., T.T, J.I., S.F.G. A.H. Writing—original draft preparation: K.S., T.T., T.J.; Writing—review and editing: K.S., K.L., T.T., M.J., J.I., A.H., S.M., K.M., M.K.E., S.J.M., M.A.P., E.V.; Prepared figures: T.J., T.T., K.S., A.H. Funding acquisition: M.P. and E.V. All authors critically revised the manuscript for intellectual content and approved the final version for publication.

Funding

The European Union supported this research through the European Regional Development Fund (Project No. 2014-2020.4.01.15-0012) and a team grant from the Estonian Research Foundation (PRG 685).

Declarations

Competing interests

The authors declare no competing interests.

Additional information

Supplementary Information The online version contains supplementary material available at https://doi.org/10.1038/s41598-024-73358-z.

Correspondence and requests for materials should be addressed to K.S.